NUMERICAL MODELING OF TWO-PHASE TURBULENT FLOWS IN COMBUSTION CHAMBERS

I. N. Gusev and L. I. Zaichik

UDC 532.517.4:532.529:662.9

It is of great practical interest to develop methods for modeling mathematically the processes occurring when fossil fuels are burned in combustion chambers. In the first works in this direction, performed at the beginning of the 1970's, attention was concentrated primarily on the analysis of gas combustion chambers, which can be described on the basis of comparatively simple physical schemes. Now, computers make it possible, in principle, to model boiler plants operating on pulverized coal. The main difficulty in the formalization of the combustion and heat and mass transfer processes in combustion chambers of this type stems from the fact that the presence of a dispersed (solid) phase and the interaction of this phase with a gaseous medium must be taken into account adequately.

There exist two alternative methods for describing the dispersed phase. The first method, Lagrange's method, is based on the calculation of individual trajectories of particles having different initial coordinates and velocities. The back effect on the carrying phase is taken into account through corresponding source terms, which determine the interphase transfer of mass, momentum, and energy. This method, described systematically in [1], has been extended to a wide class of two-phase flows. Examples of the applications of this method to the problems under consideration are in the work [2-4]. The computing resources required increase significantly when any attempt was made to take into account, on the basis of this approach, the stochastic character of the motion of finely dispersed fractions [5], since a quite representative ensemble of particles must be introduced in order to obtain the statistical information.

The second (Eulerian) approach is based on the continuous representation of an ensemble of particles and therefore make it possible to use the same numerical algorithms for both dispersed and carrying phases. However two fluid models [6] have not found applications in calculations of combustion chambers because the number of equations required increases significantly. In the existing publications [7, 8], the analysis is limited to equations of the diffusion type and the motion of the particles is identified with propagation of inertialess impurity in turbulent flows.

In the present paper we develop a model that makes it possible to take into account inertial effects together with convective transport and diffusion. The equations describing particle transport, under the assumption that the deviations of the particle velocities from the gas velocity is small, reduce to a single equation for the concentration.

1. The motion of a gas-dispersion system is described, on the basis of the theory of mutually interpenetrating media [9], taking into account the combustion of the particles, by the following equations:

$$\frac{\partial \rho_1}{\partial t} + \frac{\partial \rho_1 U_k}{\partial x_k} = \varkappa; \tag{1.1}$$

$$\frac{\partial \varphi}{\partial t} + \frac{\partial \varphi V_k}{\partial x_k} = -\frac{\varkappa}{\rho_2}; \tag{1.2}$$

$$\frac{\partial \rho_1 U_i}{\partial t} + \frac{\partial \rho_1 U_i U_k}{\partial x_k} = -\frac{\partial p}{\partial x_i} + \frac{\partial \sigma_{ik}}{\partial x_k} + \rho_1 g_i - \rho_2 \varphi F_i - \varkappa V_i; \tag{1.3}$$

$$\frac{\partial \varphi V_i}{\partial t} + \frac{\partial \varphi V_i V_k}{\partial x_k} = \varphi (g_i + F_i) - \frac{\varkappa V_i}{\rho_2}. \tag{1.4}$$

Moscow. Translated from Prikladnaya Mekhanika i Tekhnicheskaya Fizika, No. 2, pp. 116-122, March-April, 1992. Original article submitted October 17, 1989; revision submitted January 30, 1991.

0021-8944/92/3302-0257$12.50

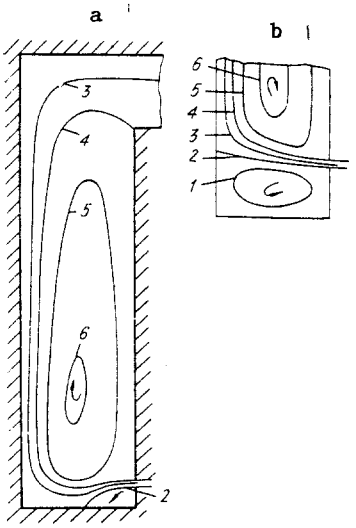

Fig. 1

Here φ is the volume concentration of the dispersed phase ($\varphi \ll 1$); ρ_1 and ρ_2 = const and U_i and V_i are the density and components of the velocity vector, respectively, of the gas and solid phases; p is the pressure; σ_{ik} is the viscous stress tensor; g is the acceleration of gravity; and $\varkappa$ is the combustion velocity of the particles. Since $\rho_2 \gg \rho_1$, the acceleration of the particles due to interphase interaction is determined only by the aerodynamic resistance force $F_i = (U_i - V_i)/\tau$; $\tau = \rho_2 d^2/18\rho_1\nu$ is the dynamic relaxation time in the case of Stokes flow past a particle; d is the effective diameter of the particles; and ν is the kinematic viscosity.

The equation of motion for the flow as a whole is obtained from Eqs. (1.3) and (1.4):

$$\frac{\partial(\rho_1 U_i + \rho_2 \varphi V_i)}{\partial t} + \frac{\partial(\rho_1 U_i U_k + \rho_2 \varphi V_i V_k)}{\partial x_k} = \\ = -\frac{\partial p}{\partial x_i} + \frac{\partial \sigma_{ik}}{\partial x_k} + (\rho_1 + \rho_2 \varphi) g_i. \tag{1.5}$$

We now average, by Favre's method [10], over realizations of the turbulent process using as the weight factors ρ_1 for the velocity of the gas phase and φ for the solid phase. Equations (1.1), (1.2), (1.4), and (1.5) assume the following form:

$$\frac{\partial \langle\rho_1\rangle}{\partial t} + \frac{\partial \langle\rho_1\rangle \langle U_k\rangle}{\partial x_k} = \langle\varkappa\rangle; \tag{1.6}$$

$$\frac{\partial \langle\varphi\rangle}{\partial t} + \frac{\partial \langle\varphi\rangle \langle V_k\rangle}{\partial x_k} = -\frac{\langle\varkappa\rangle}{\rho_2}; \tag{1.7}$$

$$\frac{\partial \langle\varphi\rangle \langle V_i\rangle}{\partial t} + \frac{\partial \left[\langle\varphi\rangle \left(\langle V_i\rangle \langle V_k\rangle + \langle v_i' v_k'\rangle\right)\right]}{\partial x_k} = \\ = \langle\varphi\rangle g_i + \frac{\langle\varphi\rangle (\langle U_i\rangle - \langle V_i\rangle) + \langle\varphi u_i'\rangle}{\tau} - \frac{\langle\varkappa V_i\rangle}{\rho_2}; \tag{1.8}$$

$$\frac{\partial (\langle\rho_1\rangle \langle U_i\rangle + \rho_2 \langle\varphi\rangle \langle V_i\rangle)}{\partial t} + \frac{\partial \left[\langle\rho_1\rangle \left(\langle U_i\rangle \langle U_k\rangle + \langle u_i' u_k'\rangle\right)\right]}{\partial x_k} + \\ + \frac{\partial \left[\rho_2 \langle\varphi\rangle \left(\langle V_i\rangle \langle V_k\rangle + \langle v_i' v_k'\rangle\right)\right]}{\partial x_k} = -\frac{\partial \langle p\rangle}{\partial x_i} + \frac{\partial \langle\sigma_{ik}\rangle}{\partial x_k} + (\langle\rho_1\rangle + \rho_2 \langle\varphi\rangle) g_i. \tag{1.9}$$

In order to expand the correlations $\langle\varphi u_i'\rangle$ and $\langle v_i' v_k'\rangle$ we specify the two-dimensional correlation function for a homogeneous stationary field of turbulent pulsations [11]:

$$\langle u_i'(t_1) u_k'(t_2)\rangle = \langle u_i' u_k'\rangle \left[1 - H\left(\frac{|t_1 - t_2|}{T}\right)\right]$$

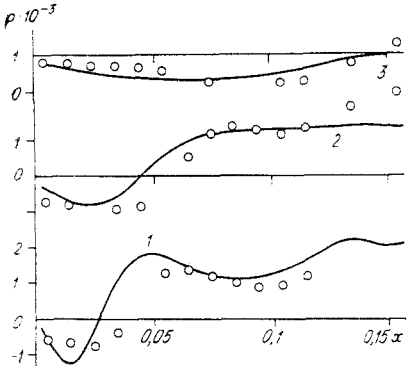

Fig. 2

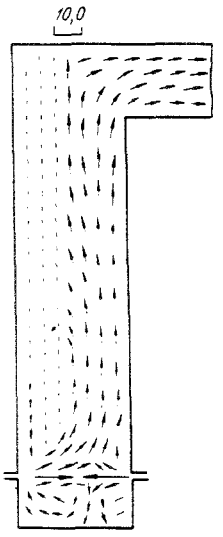

Fig. 3

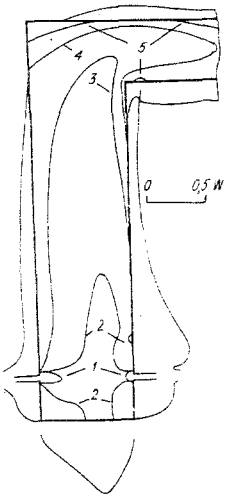

Fig. 4

where H is the Heaviside function and T is the time scale of the energy storing vortices. Then, analysis of the motion of a particle in a Gaussian random field gives [12]

$$\langle \varphi u_i' \rangle = -(T - \tau f) \langle u_i' u_k' \rangle \frac{\partial \langle \varphi \rangle}{\partial x_k}, \quad \langle v_i' v_k' \rangle = f \langle u_i' u_k' \rangle,$$

where the coefficient f = 1 − exp(−T/τ) characterizes the degree to which the solid phase is entrained into the pulsational motion of the gas.

We determine the total flux of the solid phase with the help of Eqs. (1.7) and (1.8):

$$\langle \varphi \rangle \langle V_i \rangle = \langle \varphi \rangle \langle U_i \rangle - T \langle u_i' u_k' \rangle \frac{\partial \langle \varphi \rangle}{\partial x_k} + \\ + \tau \langle \varphi \rangle \left(g_i - \frac{\partial f \langle u_i' u_k' \rangle}{\partial x_k} - \langle V_k \rangle \frac{\partial \langle V_i \rangle}{\partial x_k} - \frac{\partial \langle V_i \rangle}{\partial t} - \frac{\langle \varkappa v_i' \rangle}{\rho_2} \right), \tag{1.10}$$

which, besides transfer with the average velocity of the carrying phase and turbulent diffusion ($D_{ik} = T \langle u_i' u_k' \rangle$ is the diffusion tensor), includes an additional convective term, which is proportional to τ and takes into account a number of inertial effects. Thus, even in the absence of a concentration gradient φ the velocity of the solid phase differs from the gas velocity. The average slipping of phases, as follows from Eq. (1.10), is caused by the action of gravity, turbulent migration of particles from regions with high degree of turbulence into regions with a low degree of turbulence and inertial transport owing to deviation of particle trajectories from the gas trajectories as the gas trajectories become curved. The next to last term in parentheses is related with the existence of a finite velocity of propagation of disturbances in the dispersed phase $c_i = \sqrt{D_{ii}/\tau}$. Substituting Eq. (1.10) into Eq. (1.7) and retaining terms of only zeroth and first order in τ, we have for the stationary flow

$$\frac{\partial}{\partial x_i} \left[\left(\langle U_i \rangle + \tau \left(g_i - \frac{\partial f \langle u_i' u_k' \rangle}{\partial x_k} - \langle U_k \rangle \frac{\partial \langle U_i \rangle}{\partial x_k} \right) \right) \langle \varphi \rangle \right] = \\ = \frac{\partial}{\partial x_i} \left(D_{ik} \frac{\partial \langle \varphi \rangle}{\partial x_k} \right) - \frac{\langle \varkappa \rangle}{\rho_2}. \tag{1.11}$$

Equation (1.11) is valid for relatively small particles τ < L/ΔU, where L is the characteristic size of the flow region and ΔU is a measure of the change in velocity over a distance of the order of L.

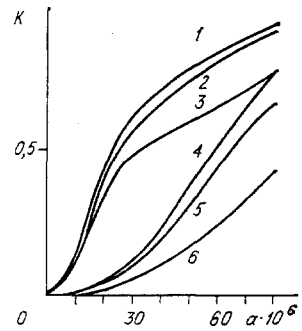

Fig. 5

The turbulent diffusion tensor D_{ik} does not depend on the particle size. This result ceases to be valid only for very large particles, whose diffusional transport is a effected by the average slipping [13]. Neglecting effects due to nongradient diffusion, we find $D_{ik} = 2\delta_{ik}kT/3$ ($k = \langle u_i' u_i' \rangle/2$ is the kinetic energy of turbulence. On the other hand, the turbulent diffusion coefficient is determined in terms of the turbulent viscosity and the turbulent Schmidt number of an inertialess impurity as follows: $D = \nu_T/Sc_T$. According to Kolmogorov's hypothesis $\nu_T = C_\mu k^2/\varepsilon$, where ε is the rate of dissipation of turbulent energy and C_μ is a constant of the turbulence model. Hence we obtain an expression for the turbulence time scale $T = (3C_\mu/2Sc_T) \times (k/\varepsilon)$.

Since in the applications under consideration the mass concentration of the solid phase is significantly lower than that of the gas phase, we include in the momentum balance equation of the two-phase system (1.9) only the pulsational slipping of the phases and we neglect the average slipping:

$$\frac{\partial}{\partial x_k}[(\langle \rho_1 \rangle + \rho_2 \langle \varphi \rangle)\langle U_i \rangle \langle U_k \rangle] = -\frac{\partial \langle p \rangle}{\partial x_i} + \\ + \frac{\partial \langle \sigma_{ik} \rangle}{\partial x_k} - \frac{\partial}{\partial x_k}[(\langle \rho_1 \rangle + f\rho_2 \langle \varphi \rangle)\langle u_i' u_k' \rangle] + (\langle \rho_1 \rangle + \rho_2 \langle \varphi \rangle) g_i. \tag{1.12}$$

The standard k–ε model of turbulence is employed to determine the one-point correlations of the velocity pulsations of the carrying phase [14].

2. Questions concerning the interaction of pulverized coal and the mineral part of the fuel with the combustor surfaces were studied in [3, 4] in the Lagrangian representation. In the present paper we study the aerodynamic aspect of the scaling problem. According to [12, 15], the particle flux onto the wall is determined by turbulent pulsations of particles in a direction perpendicular to the surface:

$$J_w = \langle \varphi \rangle_w \frac{1-\chi}{1+\chi}\left(\frac{2\langle v_n'^2 \rangle_w}{\pi}\right)^{1/2} \tag{2.1}$$

where χ is the probability that a particle recoils and returns into the flow.

The condition $\tau < L/\Delta U$ under which the analysis performed is valid can break down in zones near the walls, where the friction velocity u_* and the distance y up to the wall appear as natural scales. As a consequence, the average slipping increases strongly and the diffusion coefficient and energy of pulsational motion of the particles deviate from the values obtained in the homogeneous-turbulence approximation. This difficulty can be overcome by the method, proposed in [16], of transferring the boundary condition to a distance $au_*\tau$ from the wall, proportional to the free path of the particle (the constant a is set equal to 0.5). Then we obtain from the solution of Eq. (1.11) for plane-parallel flow with the boundary condition (2.1) a relation between J_w and the average concentration $\langle \varphi \rangle_0$ in the region $y_+ = yu_*/\nu = 30\text{-}100$. Analysis of the computational results for $\chi \in \{0; 1\}$ gives

$$J_w = \langle\varphi\rangle_0 u_* (1 - \chi) \frac{\min\left(2{,}5 \cdot 10^{-4}\tau_+^{2{,}5}; 0{,}25\right)}{\max\left(0{,}606; \min\left(1{,}316 - 0{,}2705 \ln \tau_+; 1\right)\right)},$$

where $\tau_+ = \tau u_*^2/\nu$.

This redefinition of the boundary condition can be incorporated well into the structure of conservative difference schemes. In particular, it has the same form as the boundary conditions employed in the method of wall functions [17]. The calculations of deposition in a circular pipe, performed using Eq. (2.2), agree well with the experimental data collected in [18]. The effect of the parameter $(1 - \chi)$ on the rate of deposition is not multiplicative and requires further detailed analysis. In addition, it is necessary to take into account additional deposition on the horizontal surfaces, occurring with the free-fall velocity τg, since in the gravitational field even totally reflecting surfaces, which are studied together with the gas layer adjacent to them, have an effective absorptivity.

3. Stationary isothermal single- and two-phase flows were calculated using Eqs. (1.6), (1.11), and (1.12), supplemented by the standard model of turbulence for a rectangular channel, shown in scale in Fig. 1. Flows with this geometry, simulating in a simplified form a combustion chamber, were investigated experimentally in [19] on a model of width 0.162 m and are two-dimensional.

The equations were approximated on a "checkerboard" grid using the control-volume method [20]. Since the diffusion of the particles occurs against background motion with a velocity independent of the distribution $\langle\varphi\rangle$ and different from the average velocity of the carrying phase, convective transport of the solid impurity through the face of the control volume also includes an inertial correction. This approximation method is more accurate than approximating the inertial term by a source, though it does increase somewhat the complexity of the computational algorithm. The profile between nodes was interpolated with a polynomial [20]. The main idea incorporated in the SIMPLE algorithm [21], employed in the present work to determine the pressure field, is the introduction of appropriate corrections, at each iteration, to the pressure which make it possible to satisfy the equation of continuity. The velocity field is refined on the basis of the computed corrections.

The boundary conditions at the entrance were prescribed by uniform profiles. A "soft" boundary condition, according to which the second derivative along the longitudinal coordinate vanishes for all quantities, with the exception of the transverse component of the velocity, was imposed at the exit. The transverse component of the velocity was assumed to be equal to zero at both the entrance and exit. The apparatus of wall functions [17], which take into account the behavior of aerodynamic fields near the wall, was used to determine the flow characteristics near the boundaries. The particle flux onto the chamber wall was related to the concentration in the first corner by means of the relation (2.2).

Two different types of flows [19], shown in Fig. 1, arise in the case of unilateral entry. The flow patterns shown were obtained with a Reynolds number of $3.3 \cdot 10^4$, determined according to the width of the nozzle and the velocity at the entrance. The lines 1-6 of the stream function, normalized to the total flow rate, were calculated with a step of 0.5 between the curves, starting with the value -0.5. For small distances between the bottom and the edge of the nozzle h = 0.03 m (Fig. 1a), the ejection of the jet, giving rise to a low-pressure region, causes the jet to become attached to the bottom (Coanda effect). The position of the bottom strongly affects the character of the flow at the bottom of the channel. Increasing h, leaving unchanged the other geometric dimensions of the channel, shifts the position of the point of attachment to the left and for some value of h it jumps abruptly onto the opposite wall. The transition from one type of flow to another, as the calculation showed, occurs at h ≈ 0.05 m. The streamlines in Fig. 1b were obtained with h = 0.065 m. Figure 2 shows the dependence of the bottom pressure p on the distance x from the right-hand wall. The experimental results were taken from [19] (lines 1-3 for h = 0.02, 0.029, and 0.065 m). The pressure peak in the first two cases is associated with the attachment of the jet near the center of the bottom. The data presented indicate that the computational results for quite complicated two-dimensional single-phase flows, characterized by the presence of circulation zones, turning points of the flow, etc., agree qualitatively and quantitatively with the experimental results.

As far as two-phase flows are concerned, it should be noted that in real power plants the flow velocity is such that the Reynolds number is approximately an order of magnitude higher than in the example studied. Nevertheless the overall structure of the aerodynamic fields is identical. For bilateral entry, because the oppositely directed jets interact with one another the character of the flow is not the same as in the case of unilateral entry. As an example, Fig. 3 shows the velocity field in a model configuration, keeping the same proportion as in Fig. 1b, but with a Reynolds number of $3.3 \cdot 10^5$, chosen according to the input parameters. The velocity at the exit from the burners was equal to 18 m/sec and the height of the combustion chamber was equal to 24 m. A stationary point of dislocation of the jet (saddle point for streamlines), below which a descending flow is formed, forms at the bottom of the chamber. Circulation zones are present above and below each burner zone, and in addition the left-hand upper zone occupies a larger fraction of the volume of the combustion chamber.

The distribution of particles with diameter $d = 4 \cdot 10^{-5}$ m for low concentrations with the given state parameters and slagged burners surfaces ($\chi = 0$) is shown in Fig. 4. The density ratio ρ_2/ρ_1 was assumed to be equal to 1670; the lines 1-5 of constant concentration, normalized to the input value, correspond to 0.8, 0.7, 0.6, 0.5, and 0.4. The highest values are observed near the burners and the decrease downstream is associated with precipitation of particles onto the wall. Concentration "tongues" indicating accumulation of particles predominantly in the flow-through part of the combustion chamber, are characteristic. Curves of the precipitation velocity W were constructed along the perimeter of the chamber. Since the calculations were performed for complete absorption, corresponding to ash particles with temperatures above the temperature of the plastic state and attaching completely to the walls, the profiles shown are majorizing profiles and permit judging only the maximum possible slagging velocity. The highest deposition velocity is achieved in sections located somewhat above and below the burner zones as well as at the bottom of the combustion chamber, where only 40% of the deposition is caused by gravitational settling, and the rest of the deposition must be attributed to turbulent transfer. Maximum deposition along the bottom occurs in the region of the downward flow. A slag-free zone, forming as a result of the decrease in u_*, is formed at the top of the combustion chamber.

Figure 5 shows curves of the total (along the perimeter) flow of precipitating particles K, scaled to the total flow rate of the dispersed phase, as a function of the diameter of the particles (curves 3 and 6 were obtained for the starting velocity field in Fig. 4 and curves 2 and 5 were obtained for the same input velocities but for the case when the fuel—air mixture was injected only from the right-hand side). The curves presented correspond to $\chi = 1$ (4-6), when particle precipitation is caused only by gravity, and $\chi = 0$ (1-3). Both types of boundary conditions lead to the same result: deposition with unilateral entry is more intensive because the flame is thrown onto the furnace screens (Fig. 1a). The integral deposition coefficient K reaches even higher values when the jet is attached to the bottom of the combustion chamber (Fig. 1b), in spite of the fact that the overall perimeter is somewhat smaller (curves 1, 4). In practice, this flow regime has an unfavorable effect on heat transfer and combustion processes. The difference between the curves referring to different values of χ makes it possible to judge the fraction of the particles precipitating onto the wall due to turbulent mechanism of deposition.

Thus the method examined in this paper makes it possible to predict the formation of deposits of finely dispersed ash particles on the combustor surfaces.

LITERATURE CITED

1. D. Megdal and V. D. Agosta, "A source flow model for continuum gas-particle flow," Trans. ASME: J. Appl. Mech., 35, No. 4 (1967).
2. B. P. Ustimenko, K. B. Dzhakupov, and V. O. Krol', Numerical Modelinging of the Aerodynamics and Combustion in Furnace and Technological Installations [in Russian], Nauka, Alma-Ata (1986).
3. V. Vrublevskaya, A. Vanik, and E. Shimchak, "Diagnostics of scaling of furnaces," Teploénergetika, No. 10 (1987).
4. F. C. Lockwood, C. Papadopulos, and A. S. Abbas, "Prediction of a corner-fired power station combustor," Comb. Sci. Tech., 58, No. 1 (1988).
5. A. D. Gosman and E. Ioannides, "Aspect of simulation of liquid fueled combustors," AIAA Paper No. 81-0323, New York (1981).

6. Crow, "Numerical models of gas flows with low particulate content (review)," Teor. Osnovy Inzh. Raschetov, No. 3 (1982).
7. K. Gorner and W. Zinser, "Prediction of three-dimensional flows in utility boiler furnaces and comparison with experiments," Comb. Sci. Teh., 58, No.1 (1988).
8. W. A. Fiveland and R. A. Wessel, "Numerical model for predicting performance of three-dimensional pulverized fuel furnaces," Trans. ASME: J. Eng. Gas Turbine Power, 110, No. 1 (1988).
9. R. I. Nigmatulin, Principles of the Mechanics of Heterogeneous Media [in Russian], Nauka, Moscow (1978).
10. W. Jones, "Models of turbulent flow with variable density and combustion," in: Methods for Calculating Turbulent Flows [Russian translation], V. Kollman, ed., Mir, Moscow (1984).
11. I. V. Derevich, V. M. Eroshenko, and L. I. Zaichik, "Effect of particles on the intensity of turbulent transport of dusty gas," Inzh.-Fiz. Zh., 45, No. 4 (1983).
12. I. V. Derevich and L. I. Zaichik, "Settling of particles from a turbulent flow," Izv. Akad. Nauk SSSR, Mekh. Zhidk. Gaza, No. 5 (1988).
13. A. A. Shraiber, V. M. Milyutin, and V. P. Yatsenko, Hydromechanics of Two-Component Flows with a Polydispersed Solid Material [in Russian], Naukova Dumka, Kiev (1980).
14. W. Rody, "Models of turbulence of the surrounding medium," in: Methods for Calculating Turbulent Flows [Russian translation], V. Kollman, ed., Mir, Moscow (1984).
15. K. R. Naqvi, K. J. Mork, and S. Waldenstrom, "Reduction of Fokker–Planck equation with an absorbing or reflecting boundary to the diffusion equation and radiation boundary condition," Phys. Rev. Lett., 49, No. 5 (1982).
16. S. K. Friedlander and H. F. Johnstone, "Deposition of suspended particles from turbulent gas streams," Ind. Engng. Chem., 49, No. 7 (1957).
17. B. E. Launder and D. B. Spalding, "The numerical computation of turbulent flows," Comp. Meth. Appl. Mech. Eng., 3, No. 1 (1974).
18. D. D. McCoy and T. J. Hanratty, "Rate of deposition of droplets in annular two-phase flow," Int. J. Multiphase Flow, 3, No. 4 (1977).
19. S. V. Alekseenko, M. Ya. Protsailo, and A. V. Yurlagin, "Investigation of turbulent fluid flow in a rectangular channel with lateral inputs," Izv. Sib. Otd. Akad. Nauk SSSR, Ser. Tekh. Nauk, No. 7,(2), (1988).
20. S. Patankar, Numerical Methods for Solving Problems in Heat Transfer and Fluid Dynamics [Russian translation], Énergoatomizdat, Moscow (1984).
21. S. V. Patankar and D. B. Spalding, "A calculation procedure for heat, mass and momentum transfer in three-dimensional parabolic flows," Int. J. Heat Mass Transfer, 15, No. 10 (1972).